Accuracy vs Speed: Evaluation of tradeoffs in atmospheric correction methods

Brian Cairns[a]*, Barbara E. Carlson[b], R. Ying[a], J. Laveigne[c]
[a]Columbia University, [b]NASA GISS, [c]SpecTIR Corp.

ABSTRACT

In this paper tradeoffs between speed and accuracy for the atmospheric correction of hyperspectral imagery are examined. Among the issues addressed are: the use of scattering calculations on a sparse spectral grid and consequent accuracy and speed tradeoffs; methods for minimizing the required number of quadrature points in multiple scattering calculations; effects of the vertical profiles of aerosols and absorbing gases on atmospheric correction; and efficient approaches for including the effects of sensor variability, or imperfections, on atmospheric correction.

Keywords: Atmospheric correction, multiple scattering

1. INTRODUCTION

The development over the last decade of remote sensing instrumentation that can simultaneously acquire imagery and the spectra of each pixel in the image has led to the need for fast and accurate atmospheric correction methods. As computers become faster there is less and less need to use "Empirical Line Methods" and most current efforts are oriented towards the use of accurate calculational techniques that have been speeded up in some fashion[1,2]. The major sources of uncertainty in performing atmospheric correction are water vapor and aerosols. It is therefore necessary to include water vapor and aerosols in the atmospheric correction calculations as accurately as possible. In the following we describe a calculational approach to atmospheric correction that is fast, accurate and simple such that it should be possible in future to perform atmospheric correction of hyperspectral data in the air, or at a ground terminal that is receiving the hyperspectral data from an aircraft[3]. This method can use either aerosols[4] and water vapor[1,2,5,6] derived from the hyperspectral data, or information from other ground-based[7], or airborne sensors[8].

2. METHODOLOGY

2.1 Overview of the problem

The radiance that is measured at the top of the atmosphere by a high spatial resolution (narrow field of view) instrument in a particular spectral channel, j, is given by the expression

$$I_j = \frac{\mu_0}{\pi \Delta\lambda_j} \int_{\Delta\lambda_j} r_j(\lambda) F_0(\lambda) R_A(\lambda) d\lambda \qquad (1)$$

where r_j is the (properly normalized) spectral response in channel j, F_0 is the solar flux at the top of the atmosphere and R_A is the reflectance of the atmosphere-surface system. In this discussion we are interested in the approximations that can be made to simplify the calculation of the atmospheric correction for an atmosphere with absorption by gaseous lines. For, the sake of simplicity we shall reserve discussion of the adjacency effect to an Appendix since this effect can, to a large extent, be separated from issues of spectral resolution and accuracy.

We shall first discretize the response function of the instrument such that the change in response over any one of these discrete intervals is relatively small. In the case of typical hyperspectral instruments a reasonable discretization within the spectral responsivity of a given band is one nm. The expression given above can then be written as

$$I_j = \frac{\mu_0}{\pi N} \sum_{l=1}^{N} r_j^l F_0^l \frac{1}{\delta\lambda_l} \int_{\delta\lambda_l} R_A(\lambda) d\lambda \qquad (2)$$

where

* bc25@columbia.edu; phone 1 212 678-5625; fax 1 212 678-5552; http://www.giss.nasa.gov/data/rsp_air; NASA GISS, 2880 Broadway, New York, NY 10025.

Algorithms and Technologies for Multispectral, Hyperspectral, and Ultraspectral Imagery VIII, Sylvia S. Shen, Paul E. Lewis, Editors, Proceedings of SPIE Vol. 4725 (2002)

$$F_0^l = \frac{\int F_0(\lambda) r_j(\lambda) d\lambda}{\int_{\delta\lambda_l} r_j(\lambda) d\lambda} \quad \text{and} \quad r_j^l = \frac{\int r_j(\lambda) d\lambda}{\delta\lambda_l} \tag{3}$$

The instrument response has been removed from the spectral integration over variations in atmospheric scattering and absorption, such that the calculation of atmospheric correction has been separated from the convolution over the specific instrument response function. This allows adjustments to the integration over instrument spectral response for "smile", temperature, or shock, induced shifts, or other instrumental problems to be functionally and operationally separated from the effects on the observations that are caused by the atmosphere. The principal problem in atmospheric correction is therefore the calculation of the atmospheric properties integrated over some suitably chosen spectral integral $\Delta\lambda_l$. The properties that are required from these calculations are defined in the usual form of the equation that is used to model the effects of the atmosphere on the observed reflectance

$$R_{obs} = R_A + T_2 \frac{R_S}{1 - sR_S} \tag{4}$$

where R_A is the atmospheric reflectance, T_2 is the two way transmission including both diffuse and direct beam transmission, R_S is the surface reflectance and s is the spherical albedo of the atmosphere when illuminated by the surface. It is important to note that when absorption is present and the atmosphere is vertically inhomogeneous the spherical albedo of the atmosphere is substantially different for illumination from below compared to when it is illuminated from above. We shall now concentrate on simplifications for calculating the atmospheric reflectance, the two way transmission and spherical albedo of the atmosphere when illuminated by the surface over narrow spectral bands.

2.2 Scattering

If only scattering affected the observations from hyperspectral sensors then there would be little point in calculating the atmospheric properties at the resolution of the sensor, since aerosol and molecular scattering have smoothly varying spectral signatures that can be calculated at coarse resolution and then interpolated to the required spectral interval. In Figure 1 we show that relative errors caused by the spectral interpolation of reflectance over the range 400 nm to 2500 nm are small (<1%) even with only 43 baseline spectral reflectance calculations.

The other issue with regard to the speed and accuracy of multiple scattering calculations is the number of quadrature points that are used. In Figure 2 we show the results from using the doubling/adding method[9] with extra points at the required solar zenith and view zenith angles to perform multiple scattering calculations with varying numbers of quadrature points. We also did similar calculations using the doubling adding method but also separating out the single scattering and adding it back in exactly at the end of the calculation[10]. In both cases it appears that if extra points are used for the specific view geometry of the sensor the required number of quadrature points can be reduced to only 5, or 6. Additional reductions in computational time can be obtained by automating[11] the stopping points for doubling calculations. Although the "trick" of removing single scattering from the results and then adding it back in exactly does not provide significant benefits in this case it is helpful if interpolation of view angles from those that are actually calculated is required (e.g. for wide field sensors).

The conclusions that can be drawn from these results are that, if it is possible to decouple absorption and scattering more accurately than simply separating the two processes then scattering calculations would only be required on a coarse spectral grid, and that if "extra" quadrature points are used multiple scattering properties can be calculated very rapidly and accurately for any given data set, using the best possible estimates for optical depth and scattering phase function available, rather than using pre-calculated tables of scattering properties.

2.3 *k* distributions

The only atmospheric property that varies rapidly on a one nm spectral scale is absorption by gases. The most accurate calculations of atmospheric reflectance use calculations at a sufficiently high spectral resolution that the absorption lines of the gases are resolved. These are called line-by-line calculations. The *k* distribution is based on a reorganization of the spectral integral such that it becomes an integral over the fraction of lines with a given strength. The *k* distribution and its properties have been discussed at length elsewhere[12,13].

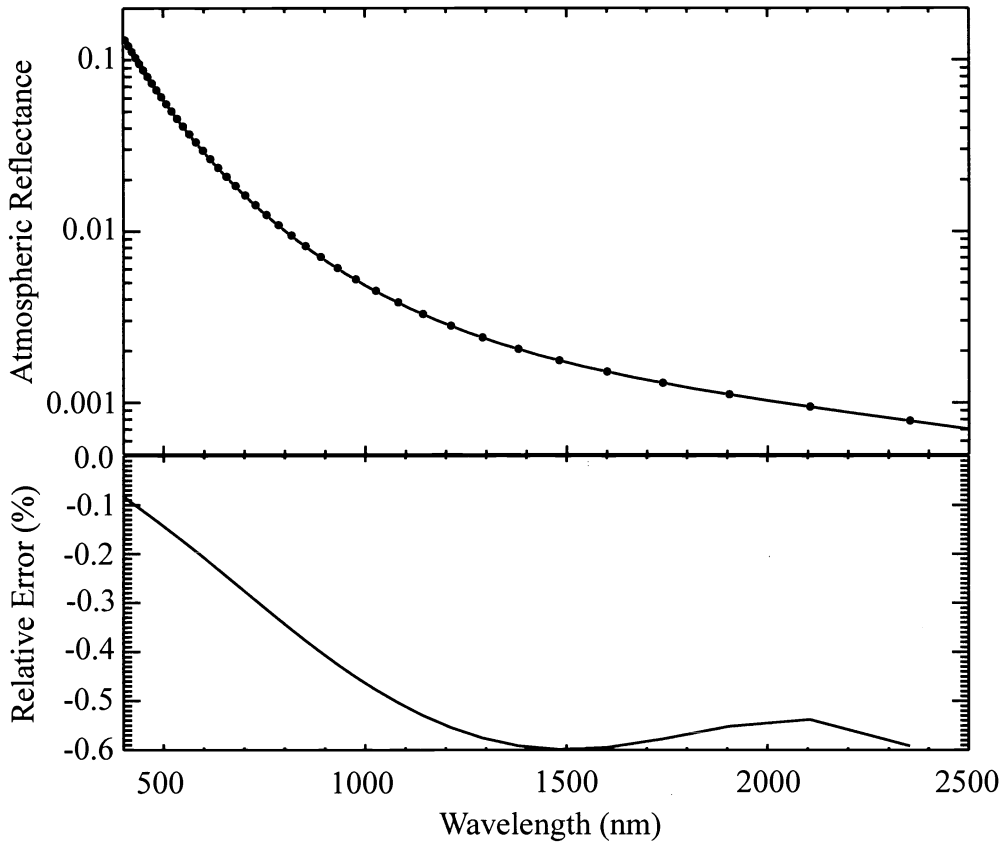

Figure 1. a) Reflectance for an atmosphere containing molcules and aerosols (optical depth of 0.1 at 550 nm) calculated at 500cm^{-1} resolution from 400 nm to 2500 nm (line), together with the calculated reflectance at the midpoints, in frequency, of this discretization (filled circles). b) Relative error in interpolating the calculations with 500 cm^{-1} spacing from 400 nm to 2500 nm to the midpoints of this spectral discretization.

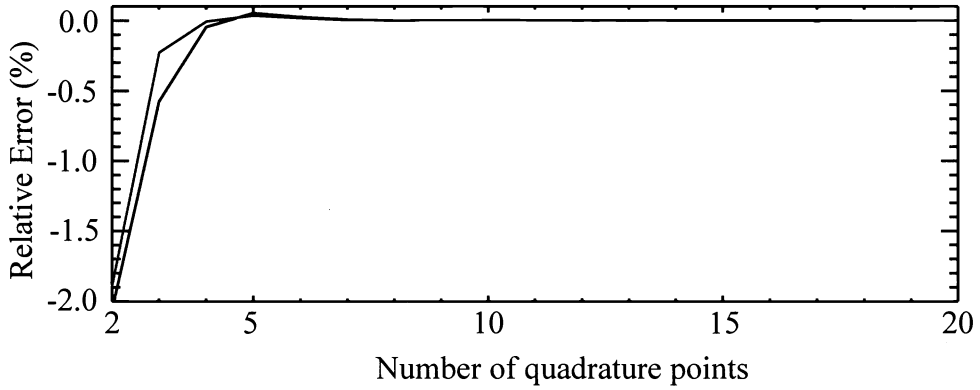

Figure 2 Relative reflectance error as a function of the number of quadrature points when the reflectance is calculated at a pair of extra points (lower curve) and when the reflectance is calculated at a pair of extra points and single scattering is added back in exactly (upper curve).

In Figure 3) below it is shown how the *k* distribution works. On the left is shown the variation of the O_2 column absorption with wavelength in the 760 nm spectral interval. The figure on the right shows the cumulative histogram of absorption coefficients in this same spectral interval.

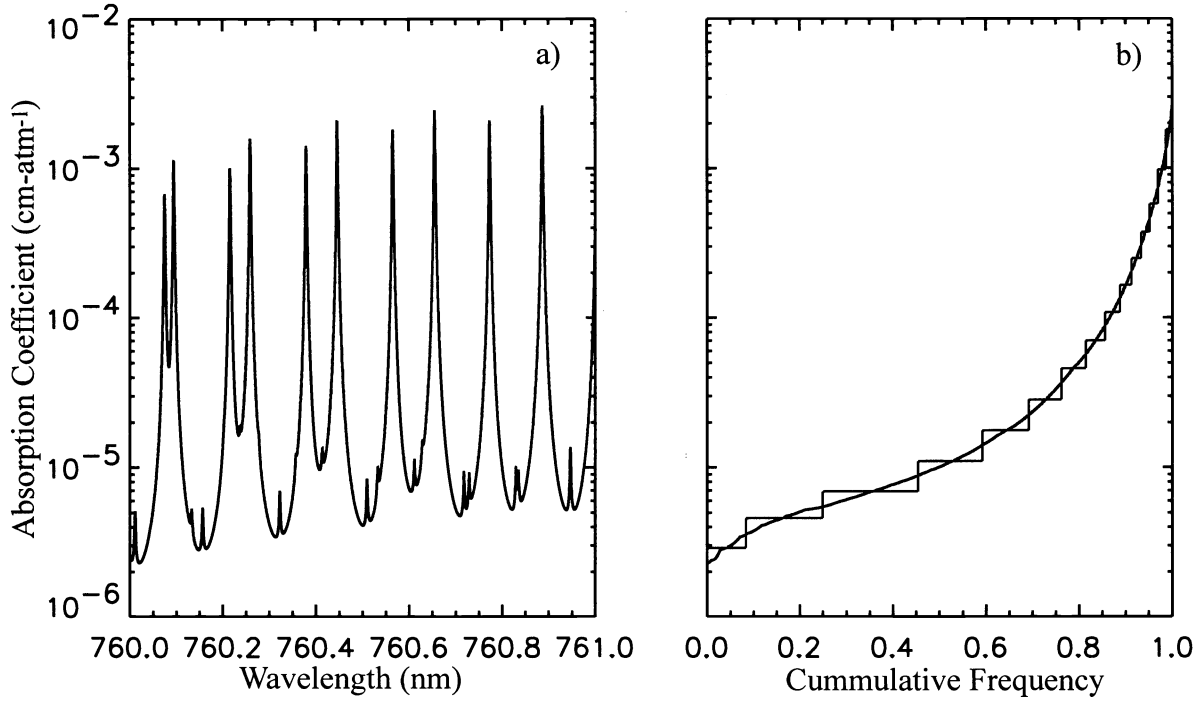

Figure 3. a) Variation of the O_2 absorption coefficient as a function of wavelength between 760 and 761 nm in the A-band and b) plotted as a cumulative histogram with a set of k values based on 15 discretization intervals.

Evidently it is more accurate, given a limited number of discretization intervals, to discretize the distribution on the right, provided there is no sub-band variation of other atmospheric properties such as scattering. For polydisperse scatterers the spectral variation of scattering properties is smooth on a one nm scale and can be considered to be essentially constant within such a bandwidth. Thus, the spectral integration shown in Eq. (2) can be transformed into an integration over absorption strength.

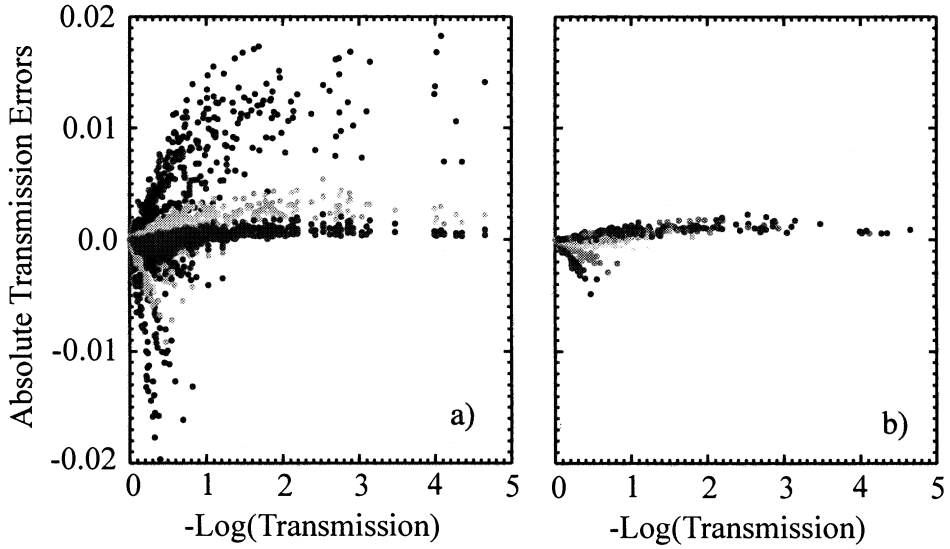

Figure 4. The figures above show the absolute error of k distribution calculations of transmission with 1 nm resolution compared with line by line calculations for water vapor over the spectral range from 900 to 1000 nm. The comparison is over a range of water vapor total column amounts from 0.25 precipitable cm to 16.0 precipitable cm. The k distributions

were tuned to provide exact results for a column amount of water of 2.0 precipitable cm with an airmass of 2.5 (i.e. 5 precipitable cm is the effective column amount). This airmass was chosen as being indicative of a nadir viewing sensor with solar zenith of 48°. a) Transmission accuracy for *k* distributions with 5, 10, 15 and 20 intervals shown in blue, green, red and purple respectively. b) Transmission accuracy as a function of water vapor amount for *k* distributions with 15 intervals, where the water vapor amounts are 0.25, 0.5, 1.0, 2.0, 4.0, 8.0 and 16.0 precipitable cm shown in blue, mauve, turquoise, green, red, orange and purple respectively.

2.4 Accuracy of *k* distributions

As noted by Lacis and Oinas[10] the *k* distribution can be tuned to provide exact transmission values for a particular absorber amount. The absorber amount for which the *k* distributions are exact in this application uses an airmass of 2.5 (e.g. nadir viewing and solar zenith angle of 48°) and column absorber amounts of 2 precipitable cm of water vapor with typical column amounts for the well mixed gases and CO. If it is required that the *k* distribution be accurate over a wide range of absorber amounts then a reasonable number of absorption, or g, intervals must be used. The number of required absorption intervals is determined by the required accuracy and range of absorber amounts over which this accuracy is to be maintained. In Figure 4 it is shown that the absolute errors in direct beam tranmission can be kept below 0.005 over a wide range of absorber amounts using 15 absorption intervals.

2.5 Vertical distribution of absorption

We have not, thus far, discussed the vertical variation of absorption. The monotonic ordering of absorption coefficient strengths in the *k* distributions in each vertical layer implicitly preserves the monochromatic structure of the atmosphere at different pressure levels, thus simulating the monochromatic structure of the atmosphere at a fraction of the line-by-line computing cost. For the purposes of atmospheric correction this method would require the calculation of the reflectance and transmittance in each layer for each absorption interval. This can be represented by the equation

$$R_A = \sum_i \left(\sum_z R_A^z(k_i u) \right) \Delta g_i \qquad (4)$$

where the summation over vertical layers (z) is a formalism indicating an adding calculation[9] and R_A is the atmospheric reflectance. Here we have suppressed the dependencies of reflectance on other atmospheric properties and it should be noted that the same summations are required for all the other quantities used in atmospheric correction. Although the use of the *k* distributions in each vertical layer provides very high accuracy compared with line-by-line calculations, it is not always necessary to have such accuracy for atmospheric correction. In particular, atmospheric correction only requires that the upwelling radiance be simulated accurately at the top of the atmosphere, or at the flight level of an aircraft. The radiance at the centers of absorption lines, or in this case the *k* values with the strongest absorption, will contribute a negligible amount to the band integral since most of this radiation is absorbed. The majority of the observed upwelling radiance will therefore come from the wings of absorption lines. The wings of spectral lines in the troposphere, where the majority of the gaseous absorption occurs, are Lorentzian and the absorption strength in the wings is therefore proportional to the line strength and the line width. The combined dependence of the line width, the vibrational partition function, the rotational partition function and the lower state population probability on temperature is weak and the dominant dependency is therefore a linear dependence on pressure, at least for water vapor absorption.

In Figure 5, below, the variation of normlized *k* value with pressure for particular g intervals is shown for all the *k* distributions in the spectral range from 920 to 930 nm. The *k* intervals are ordered from smallest to largest, and the lower *k* intervals should therefore correspond to either line wings, or the centers of very weak lines, while the higher *k* intervals will correspond to line centers. As discussed above, those *k* intervals that come from line wings should have a linear dependence on pressure of their *k* values as can be seen for the third and seventh *k* interval. Those *k* intervals that are dominated by contributions from line centers will not have such a simple dependence on pressure as can be seen for the eleventh and fifteenth *k* intervals. However, since for the purposes of atmospheric correction we are not interested in the vertical distribution of heating, those *k* intervals which contribute the majority of the transmitted and reflected light are the ones which are of relevance. As can be seen from the annotations on Figure 5 the fraction of transmitted light contributed by the eleventh and fifteenth *k* intervals is small compared with that contributed by the third and seventh *k* intervals.

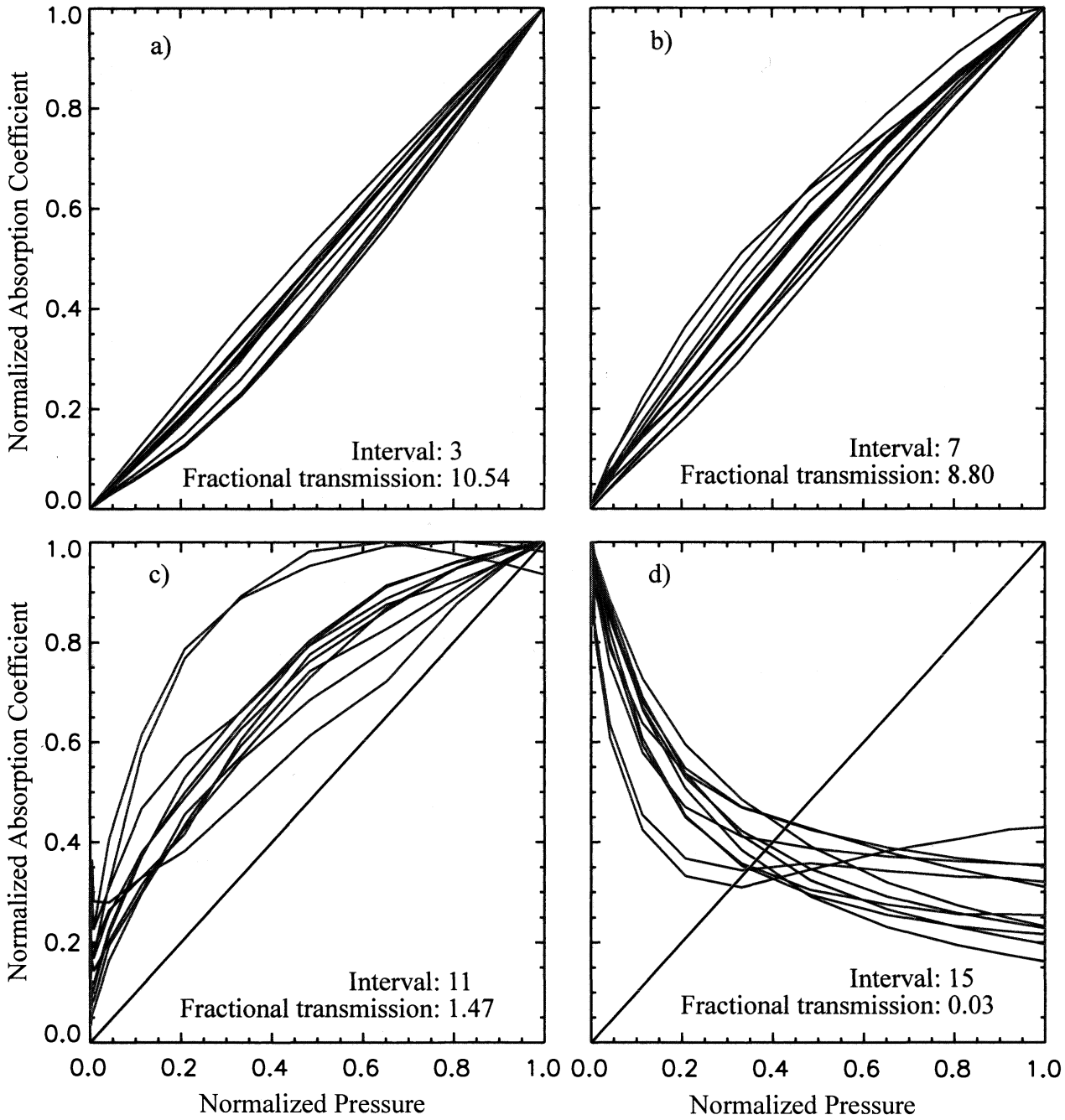

Figure 5. These figures show the variation of *k* value with pressure for the a) third, b) seventh, c) eleventh and d) fifteenth *k* absorption interval for all the one nm spectral bands between 920 and 930 nm.

This feature of absorption and the consequent insensitivity of atmospheric reflection and diffuse transmission to the detailed distribution of absorption with altitude near line centers suggests an alternative approach to calculating the reflectance in an absorbing band. In this approach we calculate the reflectance for multiple absorption values, that cover the range that may be expected, with a vertical distribution of the absorption that is appropriate for a particular gas, such as water vapor viz.,

$$R_A^T(\tau_{abs}) = \sum_z R_A^z(\tau_{abs} w_z) \quad \text{where} \quad w_z = \frac{u_z p_z}{\sum_z u_z p_z} \tag{5}$$

with u_z being the profile of absorber amout and p_z the pressure for the vertical discretization used in the multiple scattering calculations. We found that using 21 absorption optical depths log-linearly spaced from zero absorption to 10^5 provided sufficient range and accuracy. The reflectance for a particular spectral band can then be calculated by interpolating the pre-calculated multiple absorption optical depths to the column absorption values required by the k distribution for that band and summing with appropriate weights i.e.,

$$R_A = \sum_i R_A^T(\tau_i)\Delta g_i \quad \text{where} \quad \tau_i = k_i u_{tot} \tag{6}$$

This approach separates the actual details of gaseous absorption from the scattering calculation, which allows the scattering calculations to be performed on the type of coarse spectral grid described in section 2.1 above and then interpolated to the spectral interval of interest. We have therefore transformed the problem of multiple radiative transfer calculations (e.g 2100 spectral intervals for calculations at 1nm spacing from 400 to 2500 nm and 15 absorption values for accurate use of k distributions) to fewer radiative transfer calculations (43 with 21 absorption values) and some simple interpolations. It should be emphasized that the k distributions used in the final summation over absorption optical depth are based on exact line by line calculations (no assumptions about temperature, or pressure dependence are made) for a 12 layer standard atmospheric profile and that the direct beam transmission is always calculated using these k distributions, which ensures the accuracy of the direct beam calculation. Other atmospheric profiles (e.g. tropical, mid-latitude winter etc., or measured) can be added as required by simply recalculating the k distributions from the corrected Hitran-96[14] data base. When lines overlap the effectively randomly overlapped approach suggested by Lacis and Oinas[13] is used.

As we showed above this interpolation approach is extremely accurate for purely scattering atmospheres, we therefore show in Figures 6 and 7 below examples of the accuracy of this approach when it is used in absorption bands.

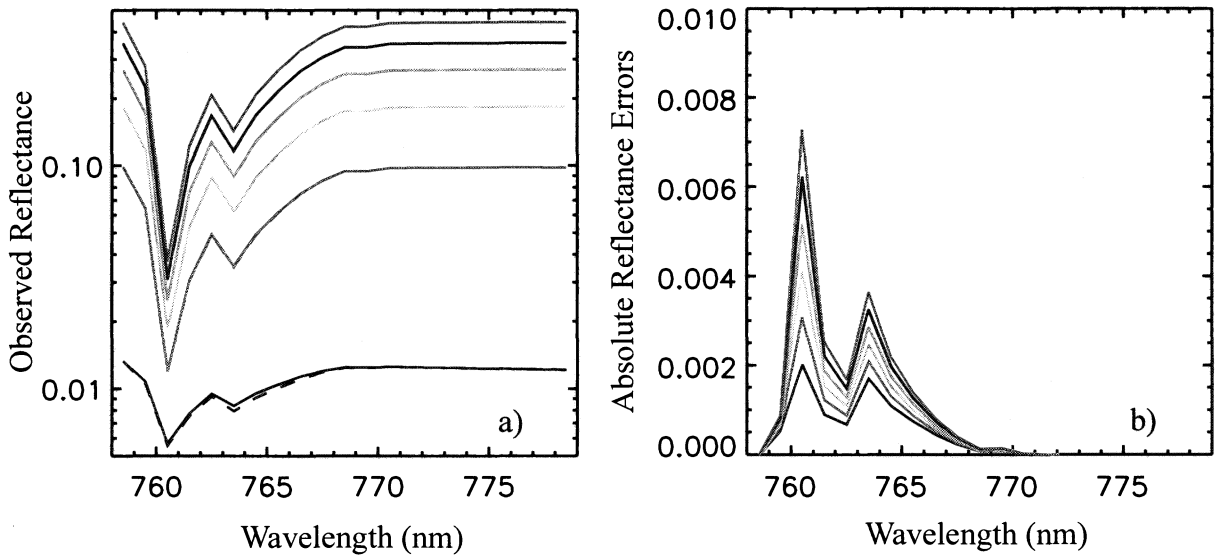

Figure 6. a) Observed reflectance calculated in the O_2 A band using exact calculations every 1 nm (solid lines) and using our approximate, spectrally interpolated with pressure weighted distribution of absorption, approach (dashed lines). The surface reflectance is Lambertian and has a value of 0.0, 0.1, 0.2, 0.3, 0.4 and 0.5 (shown as lines with increasing magnitude). b) The absolute surface reflectance error obtained when the observed reflectances simulated using the exact calculations are atmospherically corrected using the approximate approach (lines with increasing magnitude correspond to surface Lambertian reflectances of; 0.0, 0.1, 0.2, 0.3, 0.4 and 0.5).

It is apparent that the error in atmospheric correction caused by calculating atmospheric multiple scattering effects using pressure weighted absorber amounts at coarse spectral resolution that are then spectrally interpolated is quite small.

Thus, the reflectance can be pre-calculated, or calculated for the particular conditions present, with an appropriate vertical distribution of absorption which is representative of all the k intervals that make a significant contribution to the observed radiance. Over the spectral region of interest here (400-2500 nm) it is necessary to have at least two different vertical distributions of absorption, one for well mixed gases (CO, CO_2, CH_4, N_2O, O_2) and one for water vapor, since the scale heights of these gases are very different, and also to choose between these vertical distributions in spectral domains where there is line mixing. CO is treated as a well mixed gas because of the absence of readily available information that would allow for a better treatment. Since multiple scattering calculations are only required on a sparse grid, these calculations can be done beforehand and used as look-up-tables, or calculated at the time with detailed aerosol size distributions and refractive indices.

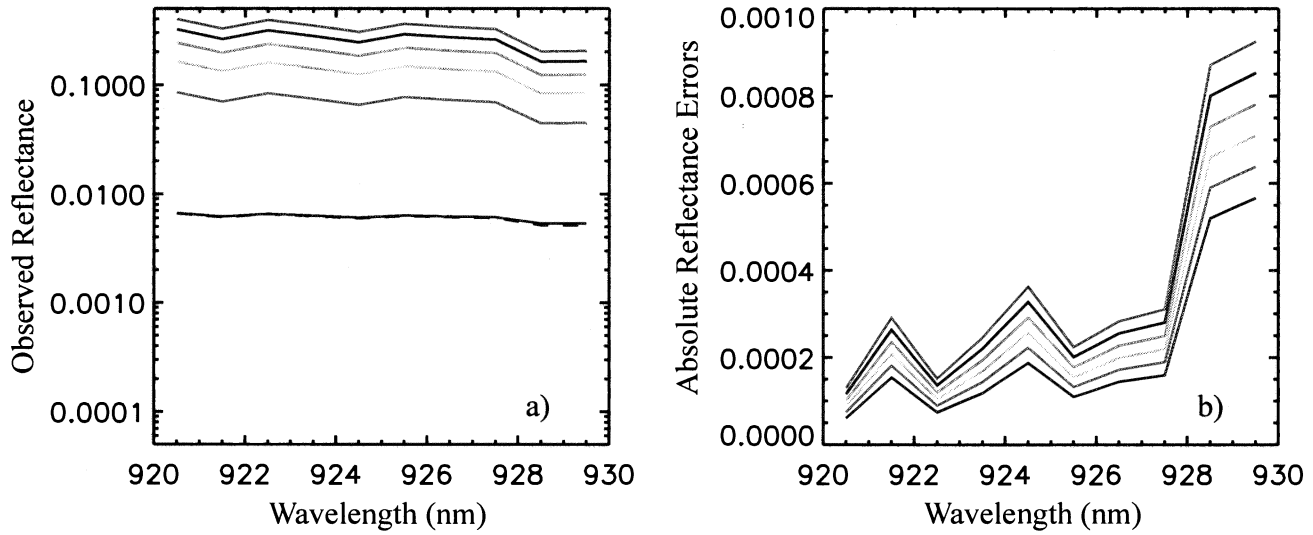

Figure 7. a) Observed reflectance calculated in an H_2O band using exact calculations every 1 nm (solid lines) and using our approximate, spectrally interpolated with pressure weighted distribution of absorption, approach (dashed lines). The surface reflectance is Lambertian and has a value of 0.0, 0.1, 0.2, 0.3, 0.4 and 0.5 (shown as lines with increasing magnitude). b) The absolute surface reflectance error obtained when the observed reflectances simulated using the exact calculations are atmospherically corrected using the approximate approach 5 (lines with increasing magnitude correspond to surface Lambertian reflectances of; 0.0, 0.1, 0.2, 0.3, 0.4 and 0.5).

2.5 Other issues

As well as line absorption it is also necessary to include absorption from continuum features in the calculation of the atmospheric correction functions. Since absorption by ozone is predominantly above most atmospheric scattering the absorption by this gas and NO_2 are treated as being physically separated (i.e., above, in the stratosphere) all the scattering and they therefore only affect the direct beam transmission. Other continuum absorption features that are included in our scattering calculations, with appropriately pressure weighted vertical distributions, are the water vapor continuum[15] (self and foreign broadened) and the O_2-O_2 continuum.

3. CONCLUSIONS

The final results of the atmospheric correction calculations are the atmospheric reflectance, the spherical albedo of the atmosphere illuminated from below, two-pass direct beam transmission and two-pass diffuse transmission at one nanometer resolution that can be convolved over the instrumental response. These are shown in Figure 8 for a typical atmosphere (1 precipitable cm water vapor and optical depth of 0.1 at 550 nm). Outstanding issues that remain to be resolved are the best approach for treating mixing of lines where their absorption overlaps and the best method for dealing with adjacency effects. Maximally and randomly overlapped line absorption approximations will be tested against exact line-by-line calculations to determine the preferred approach for modeling the effects of overlapping line absorption, while alternative approaches for treating the adjacency effect are outlined in Appendix A. We expect to use forthcoming data acquisitions over Los Angeles, a highly polluted target with strong reflectance contrasts on all spatial scales, to evaluate which is the preferred method for performing adjacency correction.

The method described here to calculate the multiple scattering properties required for atmospheric correction appears to have considerable promise in terms of allowing accurate calculations to be performed very rapidly, with the potential to perform near real time atmospheric correction. A particular advantage of this approach is that because the scattering calculations and the resolution of the line absorption calculations are decoupled it is straightforward to perform calculations at any spectral resolution, provided k distributions are available at the required resolution, or line-by-line calculations from which such distributions can be calculated are available.

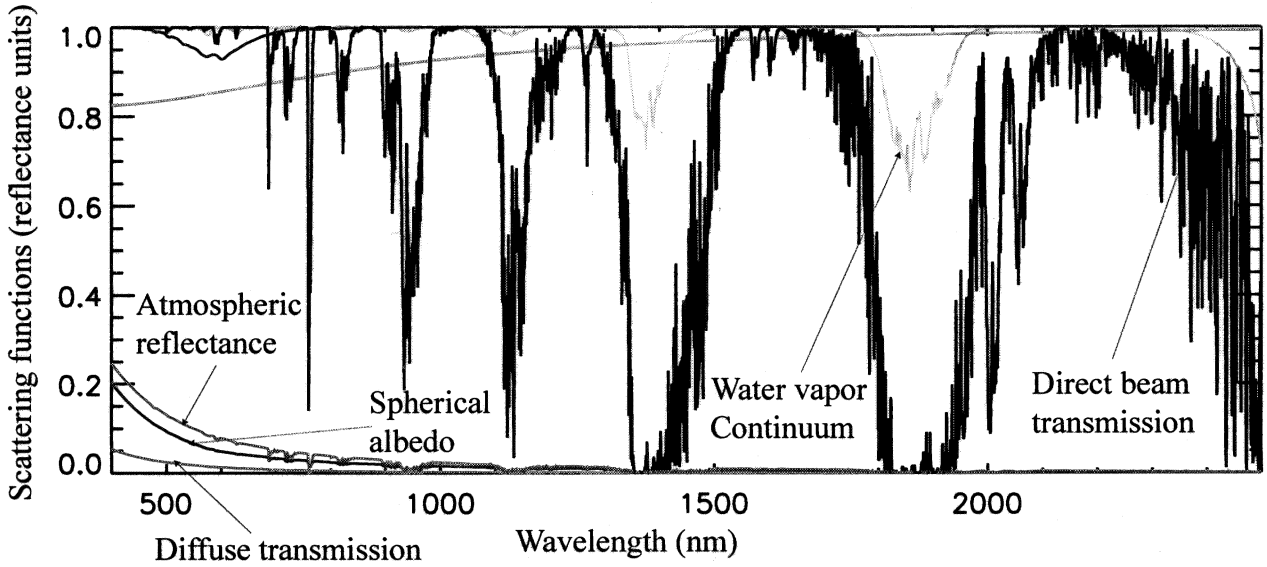

Figure 8. Atmospheric scattering and absorption properties (labelled in the figure) calculated at one nanometer resolution using 15 k intervals in each spectral band where line absorption is present.

ACKNOWLEDGMENTS

The authors would like to acknowledge support from the NASA NMP EO-1 Science Validation Team and NASA SBIR award NAS13-02005.

REFERENCES

1. Z.Qu, A. F. H. Goetz and K. B. Heidebrecht, High accuracy atmosphere correction for hyperspectral data (HATCH). Summaries of the Ninth Annual JPL Earth Science Workshop, Vol I, available at http://makalu.jpl.nasa.gov, 2000.
2. M. W. Matthew *et al.*, Status of atmospheric correction using a MODTRAN4-based algorithm. Summaries of the Ninth Annual JPL Earth Science Workshop, Vol I, available at http://makalu.jpl.nasa.gov, 2000.
3. L. A. Watts *et. al.,* Unique VIS/NIR -SWIR Hyperspectral and Polarimeter instrument suite using simultaneous polarimetry for inflight atmospheric correction of data, Proceedings of the 5th International Airborne Remote Sensing Conference, Paper # 00146, 2001.
4. Kaufman, Y. J. *et. al.,* The MODIS 2.1μm channel - Correlation with visible reflectance for use in remote sensing of aerosol, *IEEE Trans. Geo. Rem. Sens*, **35**, 1286-1298, 1997.
5. B.-C. Gao and A. F. H. Goetz, Column atmospheric water vapor and vegetation liquid water retrievals from airborne imaging spectrometer data. *J. Geophys. Res.*, **95**, 3549-3564, 1990.
6. L. Harrison *et. al.,* The rotating shadowband spectroradiometer (RSS) at the SGP. *Geophys. Res. Letts.,* **26**, 1715-1718, 1999.
7. M. D. Alexandrov, A. A. Lacis, B. E. Carlson, B. Cairns, Remote Sensing of Clouds and Atmosphere VI: Derivation of 2D fields of aerosol and trace gases parameters by integrated analysis of multi-instrument MFRSR dataset from DOE ARM Program CART site, SPIE Proc. Vol **4539**, 2001.
8. B. Cairns, M.I. Mishchenko and L.D. Travis and J Chowdhary , Aerosol retrievals over land surfaces (The Advantages of Polarization), Proceedings of AMS Annual Meeting, Albuquerque, NM, January 2001.
9. Hansen, J.E. and L.D. Travis, Light scattering in planetary atmospheres, *Space Sci. Rev.*, **16**, 527-610, 1974.

10. de Haan, J. F., P.B. Bosma and J.W. Hovenier, The adding method for multiple scattering calculations of polarized light. *Astronom.Astrophys.*, **183**, 371-391, 1987.
11. B. Cairns, B.E. Carlson, A.A. Lacis and E.E. Russell, An analysis of ground-based polarimetric sky radiance measurements, *Proc. SPIE*, **3121**, 383-393, 1997.
12. R. M. Goody and Y. L.Yung, *Atmospheric Radiation: Theoretical Basis.* pp.125-188, Oxford University, New York, 1989.
13. A. A. Lacis and V. Oinas, A description of the correlated k distribution method for modeling nongray gaseous absorption, thermal emission and multiple scattering in vertically inhomogeneous atmospheres. *J. Geophys. Res.*, **96**, 9027-9063, 1991.
14. Q. Ma and R. H. Tipping, A far line shape theory and its application to the water continuum absorption in the infrared region. I, *J. Chem. Phys.*, **95**, 6290-6301, 1991.
15. L. P. Giver, C. Chackerian Jr. and P Varanasi, Visible and near-infrared H2O line intensity correction for Hitran-96. *J. Quant. Spectrosc. and Radiat. Transfer*, **66**, 101-105, 2000.
16. E. F. Vermote et al., Second Simulation of the Satellite Signal in the Solar Spectrum (6S), 6S User Guide Version 6.0, NASA-GSFC, Greenbelt, Maryland, 1994
17. R. Richter , "Atmospheric correction of DAIS hyperspectral image data. *Proc. SPIE*, **2758**, 1996.
18. E. F. Vermote *et al.*, Atmospheric correction of visible to middle infra-red EOS-MODIS data over land surfaces: Background, Operational algorithm and validation. *J. Geophys. Res.*, **102**, 17131-17141, 1997.

APPENDIX A - ADJACENCY EFFECT

Adjacency effects are caused by light being scattered into the sensor field of view from locations at the surface other than the location that is apparently being observed by the sensor. If we assume that the atmosphere is horizontally homogeneous on scales larger than the surface variability of interest then the magnitude of the adjacency effect can be calculated if the scattering properties and amount of the aerosols, the scattering by molecules and the amount of absorbing gases are known, together with the vertical distribution of all these properties. In the following discussion it is assumed that the surface is a Lambertian reflector in order to simplify notation and presentation. A more illuminating treatment than that given in Eq.(4) is obtained by examining the upwelling radiation at the surface-atmosphere interface and its subsequent transmission through the atmosphere. The effects of the atmosphere on the observed reflectance can then be captured by a pair of equations viz.,

$$\begin{aligned} R_{obs}(\mathbf{x}) &= R_A + T_D U(\mathbf{x}) T^{\downarrow} + \int_{\Omega} T_S(\mathbf{x}-\mathbf{x}') U(\mathbf{x}') d\mathbf{x}' T^{\downarrow} \\ U(\mathbf{x}) &= R_S(\mathbf{x}) + R_S(\mathbf{x}) \int_{\Omega} s(\mathbf{x}-\mathbf{x}') U(\mathbf{x}') d\mathbf{x}' \end{aligned} \qquad \text{(A1)}$$

where T_D is the upward direct beam transmission, T_S is the scattering (or diffuse beam) transmission, U is the upwelling radiation at the surface-atmosphere interface and T is the total downwelling transmission. Functions which depend on location are indicated by the inclusion of the spatial variable **x** as an argument. In particular the reflectance of the atmosphere is now recognized as being a function that provides illumination of the location of interest that is dependent on the reflectance of the surrounding area and the diffuse transmission is also seen to allow radiation at the top of the atmosphere to come from locations other than the apparent location being viewed. The quantity that is to be inferred from the observations is the surface reflectance. The first step in the solution of this pair of equations is to retrieve the upwelling radiation, which can be done by transforming the first of Eqs. (A1) above to obtain

$$U(\mathbf{x}) + \int_{\Omega} \zeta(\mathbf{x}-\mathbf{x}') U(\mathbf{x}') d\mathbf{x}' = \frac{R_{obs}(\mathbf{x}) - R_A}{T_D T^{\downarrow}} \qquad \text{where} \qquad \zeta(\mathbf{x}) = \frac{T_S(\mathbf{x})}{T_D} \qquad \text{(A2)}$$

and then using a Fourier transform approach to the solution of a convolution equation which yields

$$U(\mathbf{x}) = \frac{1}{(2\pi)^2} \int \left[\frac{\left(\overline{R}_{Obs}(\mathbf{k}) - R_A\right)}{T_D T^{\downarrow} \left(1 + \overline{\zeta}(\mathbf{k})\right)} \right] \exp(i\mathbf{k}.\mathbf{x}) d\mathbf{k} \qquad \text{(A3)}$$

where the overbar signs indicate that Fourier transforms of these functions are being used. This result can then be substituted into the equation

$$R_S(\mathbf{x}) = \frac{U(\mathbf{x})}{\left(1 + \int_{\Omega} s(\mathbf{x}-\mathbf{x}')U(\mathbf{x}')d\mathbf{x}'\right)} \tag{A4}$$

that gives the surface reflectance in terms of the upwelling radiation. In order to make the link to other work on this subject it is worth noting that if

$$\frac{U(\mathbf{x}) - R_S(\mathbf{x})}{R_S(\mathbf{x})} << 1 \tag{A5}$$

then Eqs. (A1) above can be simplified and combined to give an expression for the observed reflectance

$$R_{obs}(\mathbf{x}) = R_A + T_D \frac{R_S(\mathbf{x})}{1 - \int_{\Omega} s(\mathbf{x}-\mathbf{x}')R_S(\mathbf{x}')d\mathbf{x}'} T^{\downarrow} + \frac{\int_{\Omega} T_S(\mathbf{x}-\mathbf{x}')R_S(\mathbf{x}')d\mathbf{x}' T^{\downarrow}}{1 - \int_{\Omega} s(\mathbf{x}-\mathbf{x}')R_S(\mathbf{x}')d\mathbf{x}'} \tag{A6}$$

that is essentially the same form as that given by Vermote *et al.*[16] and which can be used as the starting point for the correction of the adjacency effect[17,18]. The constraint given in Eq. (A5) is essentially a requirement that multiple interactions between the atmosphere and surface decrease rapidly with order of interaction, which is true for most spectral bands as long as the aerosol load is not heavy. Under these conditions there is little difference between the approximate approach to atmospheric correction contained in Eq. (A6) and the approach suggested here. Moreover, it remains an outstanding issue as to whether the more exact approach derived here, which neglects the form of the surface BRDF, is actually more accurate than simpler approaches. Nonetheless we regard this formalism as helpful in examining the types of approximations that are being made in the atmospheric correction of hyperspectral imagery and would also note that it is possible to include BRDF effects within this formalism, at the expense of increased notational and calculational complexity.